Title

Probing the surface chemistry for reverse water gas shift reaction on Pt(111) using ambient pressure X-ray photoelectron spectroscopy

Authors

Su, Hongyang
Ye, Yifan
Lee, Kyung-Jae
et al.

Publication Date

2020-11-01

DOI

10.1016/j.jcat.2020.08.017

Peer reviewed

Probing the surface chemistry for Reverse Water Gas Shift Reaction on Pt(111) using Ambient Pressure X-ray Photoelectron Spectroscopy

Hongyang Su[1,2], Yifan Ye[1,3,4], Kyung-Jae Lee[1,5], Jie Zeng[2], Bongjin S. Mun[5], Ethan J. Crumlin[1,4]*

[1] Advanced Light Source, Lawrence Berkeley National Laboratory, Berkeley, CA 94720, United States;

[2] Hefei National Laboratory for Physical Sciences at the Microscale, Key Laboratory of Strongly-Coupled Quantum Matter Physics of Chinese Academy of Sciences, Key Laboratory of Surface and Interface Chemistry and Energy Catalysis of Anhui Higher Education Institutes, Department of Chemical Physics, University of Science and Technology of China, Hefei, Anhui 230026, P. R. China;

[3] Joint Center for Artificial Photosynthesis, Lawrence Berkeley National Laboratory, Berkeley, CA 94720, United States;

[4] Chemical Sciences Division, Lawrence Berkeley National Laboratory, Berkeley, CA 94720, United States;

[5] Department of Physics and Photon Science, Gwangju Institute of Science and Technology (GIST), Gwangju 500-712, South Korea;

***Corresponding Authors:** ejcrumlin@lbl.gov

Highlights

- Reverse water-gas shift reaction process on the Pt(111) surface was first monitored using ambient pressure X-ray photoelectron spectroscopy at different gas ratios and temperatures.
- CO_2 dissociation was observed with CO and O adsorbates on the Pt(111) surface exposed to pure CO_2.
- H_2 facilitated the production of CO from CO_2 across all temperatures and decrease the initial temperature of RWGS on a platinum surface.

Abstract

Using ambient pressure XPS (APXPS), we explored carbon dioxide (CO_2) adsorption and CO_2 hydrogenation on Pt(111) single crystal surface to observe the activation of CO_2 and the subsequent reaction mechanism. In pure CO_2, we observed CO adsorbates and adsorbed oxygen on Pt(111) derived from CO_2 dissociation at room temperature. The introduction of H_2 (at a pressure ratio of 1:1 (H_2:CO_2)) increase the production of CO across all temperatures by facilitating the removal of surface oxygen. As a consequence, the surface could expose sites that could then be utilized for produce CO. Under these conditions, the reverse water-gas shift reaction was observed starting at 300 ^oC. At higher H_2 partial pressure (10:1 (H_2:CO_2)), the reverse water-gas shift (RWGS) reaction initiated at a lower temperature of 200 ^oC and continued to enhance the conversion of CO_2 with increasing temperatures. Our results revealed that CO_2 was activated on a clean Pt(111) surface through the dissociation mechanism to form adsorbed CO and O at room temperature and at elevated temperatures. Introducing H_2 facilitated the RWGS as adsorbed oxygen was consumed continuously to form H_2O, and adsorbed CO desorbed from the surface at elevated temperatures. This work clearly provides direct experimental evidence for the surface chemistry of CO_2 dissociation and demonstrates how hydrogen impacts the RWGS reaction on a platinum surface.

1. Introduction

Chemical recycling of CO_2 with H_2 has attracted substantial attention in the past decade, as it is considered a highly desirable and sustainable way to produce valuable chemical stocks and useful fuel to meet growing energy demands[1-4]. One approach involves the production of CO, which serves as an important source of syngas, used industrially for Fischer-Tropsch Synthesis, and methane, utilized as a daily-use fuel for both electricity generation and heating[5].

Pt-based catalysts have proved to be promising candidates for highly efficient CO_2 hydrogenation to selectively produce CO via reverse water gas shift (RWGS) reaction[6-8], which was one of the critical industrial reactions to control the ratio of CO/H_2 in some important process including Fischer-Tropsch synthesis, methanol synthesis and ammonia synthesis. Despite numerous experimental and theoretical works addressing Pt-based catalysts for CO_2 hydrogenation[9-12], the mechanism for CO_2 hydrogenation with Pt-based catalysts is still not clearly understood. Generally, CO_2 hydrogenation on Pt-based catalysts has been reported to proceed following the RWGS process via carboxylic (COOH) or formate (HCOO) intermediates, based on density function theory (DFT) calculations[13,14]. However, a spectroscopic study demonstrates that carbonate could be the key intermediate when certain rare-earth metal oxides serve as the support[15]. Thus, it is necessary to explore CO_2 adsorption and activation in CO_2 hydrogenation experimentally to obtain clear mechanistic insight into this reaction.

Previous studies demonstrate that CO_2 does not adsorb on a clean Pt(111) surface between 110 K to 300 K, based on ultra-high vacuum (UHV) AES, TPD, and HREELS spectroscopies; however, upon doping some alkali metal atoms like potassium, CO_2 can adsorb and dissociate on the surface[16]. Contrarily, Kaliaguine et al. observed chemisorbed CO species on Pt foil treated with CO_2 during UHV XPS experiments at 77 K[17]. Nonetheless, for most cases using conventional techniques, gas pressure was constrained under 10^{-8} torr, much lower than that in practical use. To close the pressure gap between characterization and heterogenous catalysis, additional characterization techniques have been developed to work under more real-world conditions. Ambient pressure X-ray photoelectron spectroscopy (APXPS) combined with synchrotron light sources provides a good opportunity to explore the chemical state of the catalyst and adsorbates with different probing depths and at a range of pressures (typically up to 1 torr), which can help to advance our understanding of catalytic reaction mechanisms[18-21].

Herein we report an investigation of CO_2 dissociation and hydrogenation processes on Pt (111) single crystal surfaces using APXPS. Under pressure of 40 mtorr of pure CO_2, adsorbed CO and dissociated atomic oxygen were found at room temperature, providing direct evidence for CO_2 dissociation on the Pt(111) surface. At temperatures below 150 ^oC, graphitic carbon was also observed as a product of Boudouard reaction. At elevated temperatures (greater than 150 ^oC), graphitic carbon was removed even while maintaining exposure to CO_2 alone, which we hypothesize is due to the reverse Boudouard reaction. Co-dosing H_2 gas with CO_2, opposed to exposure to CO_2 alone, increased the amount of CO adsorbates formed on Pt(111) at temperatures under 200 ^oC. When a 1:1 ratio of H_2:CO_2 (40 mtorr:40 mtorr) was introduced at temperatures higher than 300 ^oC, the RWGS was detected in mass spectra by the RGA that is integrated directly into the APXPS instrument. As we further increased the H_2 partial pressure, H_2:CO_2 = 10:1 (150 mtorr:15 mtorr), the RWGS initiated at 200 ^oC and was enhanced at elevated temperatures. Our results indicate that CO_2 exposed solely to the Pt surface dissociate to form adsorbed CO and O surface species. The introduction of H_2 promoted a reaction with the adsorbed oxygen, which was continuously consumed to form H_2O. The adsorbed H_2O and CO desorbed from the surface at elevated temperatures to open up new reaction sites and thus complete the RWGS reaction. In addition, the lower reaction temperature for the RWGS under higher H_2 partial pressure indicates that the H_2 rich environment provides more reducing conditions, which facilitate the formation of H_2O and, consequently, the RWGS reaction.

2. Experiment section

2.1. Beamline 9.3.2.

Beamline (BL) 9.3.2 at the Advanced Light Source (ALS, Lawrence Berkeley National Laboratory) is equipped with a bending magnet and grating monochromators [600 l/mm] having a total energy range between 200 eV and 900 eV (soft X-ray range). The analyzer (Scienta R4000 HiPP) pass energy was set to 100 eV, using a step of 100 meV and a dwell time of 200 ms. Under these conditions, the total resolution (source and analyzer) was equal to about 220 meV, at room temperature, for photon energies ranging between 280 eV and 660 eV (the maximum flux, around 4.5×10^{-10} photons s^{-1}, is reached at an energy of 490 eV). The incidence angle between the incoming photons and the sample surface was equal to 15^o. The XPS measurements were taken in normal emission (NE) mode, at a pressure in the experimental

chamber between UHV (1×10^{-9} torr) and 200 mtorr (in a backfilled configuration where the entire chamber is filled to the set gas pressure), while differential pumping maintained UHV conditions (~1×10^{-9}-1×10^{-6} torr) for the photoelectron analyzer. The calibration of the binding energy (BE) scale was carried out using the Au 4f photoelectron peak from a clean gold polycrystalline surface as reference ($4f_{7/2}$ BE = 84.0 eV). The Beamline, maintained under UHV to avoid contamination of optical elements, is separated from the experimental chamber by a 2-mm × 2-mm × 100-nm thick Si_3N_4 window placed at a distance of about 3.0 cm from the sample[22].

2.2. Sample preparation and APXPS Experiments.

2.2.1. Sample preparation.

Before the experiments, the APXPS chamber was baked out at 120 °C for at least 24 h, resulting in a base pressure below 1×10^{-9} torr. Each gas line, including CO_2, CO, H_2O, H_2, and O_2, was also baked for 2 h to remove residual impurities. A liquid nitrogen trap was applied to the H_2 gas line to remove any water impurities in the line. Experiments were performed using a Pt(111) single crystal purchased from MaTeck. To obtain a clean surface before each set of experiments, the sample was treated by repeated Ar^+ sputtering (2 kV, 20 mA, 60 min, $P_{Ar} = 5\times10^{-6}$ torr or 6.67×10^{-4} Pa) and annealing cycles under vacuum at around 820 °C (for 5 min in each cycle) followed by cooling in O_2 (1×10^{-6} torr or 1.33×10^{-4} Pa) between 100 and 500 °C in a preparation chamber attached directly to the main experimental chamber, which allowed the sample to be cleaned and transferred to the main chamber without breaking vacuum. This cleaning procedure was proved by Nilsson et al. as the surface order and cleanliness was confirmed through observation of a sharp (1 × 1)-Pt(111) LEED pattern[23]. This process was repeated until XPS measurements confirmed the removal of carbon and oxygen contamination on the surface.

2.2.2. APXPS Experiments.

For our APXPS experiments, the pressure of each gas was controlled by metal leak valves connected separately to the main chamber. Three gas environments were applied in the experiment including pure CO_2, H_2:CO_2 = 1:1, and H_2:CO_2 = 10:1. Notably, the condition of

H_2:CO_2 = 10:1 was used to check if there is further hydrogenated products in the more reduced environment as the methanation reaction was not easy to occur on Pt surface[13]. As CO is a product of the RWGS, careful consideration and investigations were taken to ensure that we do not have CO contamination or impurity. Survey spectra before and after the experiments were collected to eliminate any possible carbonyl species (Fig. S1). In both spectra, no obvious features for nickel carbonyl were observed, which helps us exclude the existence of carbonyl contaminations. We also compared CO_2 adsorption to very low CO exposure by collecting the time-dependent spectra during the adsorption process. It turns out that even low pressure (10^{-8} torr) yields saturation effects very quickly yet are not apparent upon the introduction of CO_2 (Fig. S2). Beam damage was also checked by moving the sample by 2 mm in each case[24]. In the experiment, we routinely performed beam damage evaluations using the following procedure. We moved the sample by 2 mm from the original position used for spectra collection and collected the XPS spectra in the new probing location. The spectra obtained at the new probing location were compared with the original spectra to check if there is beam damage. In our case, we did not observe any evidence of beam damage throughout the experiment. To give an typical example, the spectra obtained in the presence of pure CO_2 for beam damage check is shown in Fig. S3, where we didn't see obvious difference compared with the C 1s spectra shown in Fig. 1b. The result indicates that there is no beam damage effect on our experiment.

Under each condition, we collected a set of data (including C 1s, O 1s, Pt 4f, and corresponding valence band spectra) until the temperature and pressure were stable. At each given temperature it took approximately 5 min to achieve a stable temperature (±2 ^{o}C). Then, spectra were collected as function of time until two consecutive spectra with almost identical features were collected to make sure the system reached a stable condition (Fig. S4). Only after the system reaches equilibrium state did we start to collect the high-resolution spectra. For the spectra collection, the scan step size was 100 meV and one set of data took approximately 20-30 minutes to collect. The photon energy applied for C 1s and O 1s spectra was 420 and 670 eV, respectively. Pt 4f spectra were collected with both 210 eV and 340 eV (Table S1). All spectra were calibrated the Fermi edge. The Shirley background was applied for each spectrum, and a Lorentzian Asymmetric (LA) line shape was applied for the peak fitting of C 1s (LA(1.2, 2.5, 0)), O 1s (LA(2, 2, 0)), and Pt 4f (LA(1.2, 85, 70)) spectra in CasaXPS. Corresponding mass spectra

were collected by the residual gas analyzer (RGA) system attached to the second differential stage pump of the APXPS system.

2.3. Mass spectrometry data calibration.

The intensities of all species were calibrated by a subtraction of the initial background and the subsequent influence of CO_2 and H_2. A baseline was established and subtracted from our experimental results in order to remove contributions from the chamber and the boron nitride (BN) sample holder. To identify the mass spectrometer baseline for conversion products, we collected the corresponding mass spectrometry data as a function of temperature while introducing CO and H_2O gases with only the BN sample holder—i.e., without the platinum sample—in the chamber. Based on our controlled experiments, the ratio of CO/CO_2 and H_2O/H_2 was largely stable in the range of 25 °C to 550 °C. The following equation was established for the calibrated intensity,

$$I_{\text{cali.}} = I_{\text{initial}} - r \times I_{\text{gas}},$$

where r represents the ratio of CO/CO_2 or H_2O/H_2, $I_{\text{cali.}}/I_{\text{initial}}$ as the calibrated/initial intensity for the species that we calibrate, I_{gas} as the intensity for the gas species as shown and detailed in Fig. S5.

2.4.Coverage calculation.

The layer attenuation model was employed to calculate the coverage of the adsorbates of graphitic carbon and surface oxygen atoms on the surface[25]. In the calculation, C 1s spectra were used for the calculation of graphitic carbon coverage and O 1s spectra was used to calculate the coverage of surface oxygen atoms. The equation for coverage calculation was described as follows,

$$t_{ads} = \lambda_{ads} ln\left[1 + \frac{I_{ads}}{I_{sub}}\left(\frac{\lambda_{sub}\,\Phi_{sub}\,\sigma_{sub}\,N_{sub}}{\lambda_{ads}\Phi_{ads}\,\sigma_{ads}\,N_{ads}}\right)\right] \quad (1)$$

$$coverage = \frac{t_{ads}}{t_{ML}} \quad (2)$$

where t represents the thickness, λ represents the inelastic mean free path (IMFP), I represents the intensity of the peaks in the spectra, Φ represents the photoionization cross section, N

represents the atom density, σ represents the X-ray flux in the experiment. To get the electron inelastic mean free path, we referred The National Institute of Standards and Technology (NIST) Electron Inelastic-Mean-Free-Path Database: Version 1.2 to calculate the IMFP of each adsorbate. The corresponding parameters are listed in Table S2.

For the coverage calculation of CO, the intensity of CO adsorbates and Pt surface species in the Pt $4f_{7/2}$ spectra were used to calculate the coverage of CO adsorbates.[26]

3. Results and discussion

3.1. CO_2 adsorption on Pt(111) in CO_2.

Each set of experiments started with a clean Pt(111) surface. Following the cleaning procedure described above in the experimental section, according to the survey spectrum recorded with an incident photon energy of 670 eV, we observed a clean Pt surface with no evidence for C 1s or O 1s, above background, under UHV conditions (Fig. S1a).

We then proceeded to collect mass spectra and corresponding C 1s and O 1s spectra while exposing the clean Pt(111) surface to CO_2 at a pressure of 40 mtorr across a range of temperatures, from 25 ^{o}C to 540 ^{o}C (Figs. 1 and S6). All spectra were fitted with the LA asymmetric peak shape, after applying the Shirley background, and the peak assignments are summarized in Table S3. At room temperature, three main components located at binding energies of 286.8±0.1 eV, 286.0±0.1 eV and 284.0±0.1 eV were found in the C 1s spectrum after deconvolution. As previously reported[26-28], the peaks at 286.8 eV and 286.0 eV can be assigned to CO adsorbates on top sites and bridge sites of the Pt(111) surface. This assignment was nicely confirmed by the corresponding O 1s spectra, which included two feature peaks at 532.7±0.1 eV and 531.0±0.1 eV for CO adsorbates. Notably, the peak for CO adsorbates exhibited asymmetric feature in C 1s spectra. For CO adsorbates on metal surface, people usually observed peak broadenings of the molecular core level spectra in XPS[29-31]. This broadening was interpreted in terms of shake-up excitations of electron-hole pairs within a $2\pi^*$-derived resonance which is partly filled in the initial state by back-donation effects. Since the CO molecules adsorbed on the surface via the C atoms, the asymmetry feature of C 1s spectra was much more obvious than that of O 1s spectra. Apart from the two CO adsorbate peaks, a new peak located at around 530.1 eV in the O 1s spectra were identified as oxygen atoms adsorbed on the Pt surface (Figs. 1b and S7). The peak intensities of CO adsorbates were higher than those of oxygen atoms, considering the

strong affinity between Pt and CO. The remaining C 1s feature at 284.0±0.1 eV represents the graphitic carbon species on the surface[32,33]. It should be noted that in the corresponding Pt 4f spectra (Figs. S6c and S8), there was little chemical shift, compared to prior studies[34,35], for Pt 4f peaks, even though CO species adsorbed on the surface. This is due to the increased photon energy generating a Pt 4f spectrum with a larger contribution from the bulk.

To further confirm our peak assignment of CO and atomic O from CO_2 dosing, we generated CO adsorption on oxygen-covered Pt(111) surface. First, O_2 gas was introduced with a pressure of 1×10^{-6} torr for 10 min and then completely pumped out. Immediately after the oxygen was pumped out, CO dosing began, at a pressure of 1×10^{-8} ~ 1×10^{-6} torr. It is well known that oxygen molecules dissociate on Pt surfaces at room temperature, and atomic oxygen can be found on the Pt surface (Fig. S9)[36-38]. Fig. S10 showed the measured spectra after oxygen gas and CO gas exposure, and the peak positions of C 1s and O 1s spectra match well with our peak assignment of adsorbed atomic oxygen and CO under CO_2 exposure[39] in Fig. 1. Also, the existence of surface CO adsorbates and oxygen atoms confirmed our observation of CO_2 dissociation on Pt(111) at room temperature. One possible interpretation for CO_2 dissociation on the Pt surface was that the existence of excess hydrogen on the surface remarkably promoted the breaking of C-O bonds in CO_2, resulting in surmountable CO_2 dissociation at room temperature on Pt(111) surface[14].

Upon dosing CO_2 at room temperature, we continued to collect X-ray photoelectron spectroscopy and mass spectrometry data as the temperature increased to 540 ^{o}C under 40 mtorr of CO_2. Notably, in the temperature-dependent experiments, surface reconstruction was also a critical parameter which could influence the results. CO is usually considered to induce the surface reconstruction during the adsorption[40]. The reconstruction was explored previously by STM, XPS, and LEED etc. Previous studies reported that CO induced the change of terraces and steps by forming nanoclusters for Pt(332) and Pt(557) surfaces. However, for Pt(111) surface, it was reported that the nanocluster was almost invisible in the STM image even as the pressure of CO gas was higher than 10 torr[40,41], indicating the CO-induced surface reconstruction didn't happen during CO adsorption on Pt(111). Thus, we think the surface change has little influence on our experiment results. Below 65 ^{o}C, the coverage of both CO adsorbates and surface oxygen (Figs. 1b, 1c, S6a, and S6b) increased, as depicted in the histogram plot (Fig. 1d). This is due to the increase in CO adsorbates and oxygen atoms formed on the surface from CO_2 dissociation.

As we further increased the temperature to 85 ºC and higher, the CO desorption kinetics became more dominant, leading to a decrease in CO peak intensities; this observation is consistent with previously reported CO temperature-programmed desorption results on Pt(111)[42].

Upon further increasing the temperature, the peak intensity of adsorbed oxygen atoms continued to increase (Figs. 1c, 1d, S6 and S7), indicating that CO_2 dissociation accelerated at higher temperatures, in accordance with the endothermic properties for CO_2 dissociation[43]. According to the CO mass spectrum recording, the intensity was initially stable but started to become prominent at temperatures higher than 450 ºC, confirming the faster CO_2 dissociation rate at elevated temperature (Figs. 1a and S11). To eliminate the influence coming from dosed CO_2, we also calculated the intensity ratio of CO/CO_2 based on our mass spectra (Fig. 1a). The obtained CO/CO_2 ratio started to increase obviously as well as we heated the sample to the temperature higher than 450 ºC. At temperatures over 500 ºC, all feature peaks for adsorbates are discernible in the C 1s spectra (Fig. 1b). However, a small shift to lower BE for the peak representing oxygen atoms is observed, from 530.0 eV to 529.8 eV. In addition, a new peak emerged at higher binding energy (around 531.6 eV) in the O 1s spectra acquired at 450 ºC and 540 ºC (Figs. 1c and S6b), and its coverage grew from 450 ºC to 540 ºC. Given that there was no peak in the corresponding C 1s spectra, we could rule out the possibility of any C-O based species. There are several possible interpretations of this new peak, one of which assigns it as the feature peak for Pt oxide (PtO), based on the obtained XPS result[44]. Consequently, we tried to determine if there was a corresponding Pt 4f spectral feature representing PtO (Fig. S12). However, there was only a minor change to the spectral goodness of fit (from 67.6 for two peaks to 64.4 for three peaks, Fig. S12), providing neither affirmation nor exclusion for this possibility. Alternative assignments include the possibility of some O-O bond on the surface at elevated temperature. As we previously mentioned, adsorbed oxygen atoms accumulated on the surface as we increased the temperature. Therefore, the likelihood of forming O-O bonds on the surface increased as the temperature rose. Lastly, H_2O impurities in the chamber may influence the O 1s spectra by forming new species, especially at elevated temperatures. As we are unable to definitively identify this spectral feature at this time, future work will employ other techniques, such as *in operando* infrared spectroscopy, and theory to further explore this new species[45-47]. As the sample cooled, the adsorbates re-appeared (Fig. 1), and they became more obvious as the temperature dropped to room temperature, resulting in a CO coverage of ~0.19 ML that is higher

than the initial one (0.02 ML, Fig. 1d; whereas a coverage of around 0.6 ML was observed when exposed to CO alone under similar conditions, Fig. S10). These results indicate that we generated more CO on the Pt surface after it was exposed to elevated temperatures.

With the temperature rising from room temperature up to 150 °C, the peak intensity for graphitic carbon at 284.0 eV kept increasing. The formation of more graphitic carbon species could originate from the Boudouard reaction ($2CO \rightleftharpoons C + CO_2$) in the system[46,49]. As the temperature was elevated higher than 150 °C, the graphitic carbon peak intensity began to drop, mainly because of the reverse Boudouard reaction by which graphitic carbon can be oxidized by CO_2 gas in the chamber. We can observe the reaction more clearly at higher temperature, owing to the endothermic nature of the reverse Boudouard reaction[50].

3.2. CO_2 adsorption and RWGS on Pt(111) in H_2/CO_2 = 1/1.

To further investigate the CO_2 hydrogenation process on Pt(111), we simultaneously co-dosed CO_2 and H_2 into the experimental chamber, each at a gas pressure of 40 mTorr (total chamber pressure was 80 mTorr). As shown in Fig. 2, we observed the same peaks representing CO adsorbates and graphite carbon species as those in pure CO_2 gas. The primary observed difference is that the adsorbed oxygen atoms can easily react with H from H_2 dissociation on the Pt surface, even at room temperature, which renders the atomic oxygen undetectable in the O 1s spectrum (Fig. 2c).

From 25 °C to 65 °C, we observed increasing coverage for CO adsorbates, which signified that additional CO was generated on the surface (Fig. 2d). The CO coverage was calculated as ~0.24 ML at 65 °C, much higher than that in pure CO_2 (~0.04 ML, Fig. 1d), which may be due to the fact that H_2 can facilitate CO_2 dissociation by removing the residual adsorbed oxygen atoms that are blocking potentially viable active sites. Additionally, in the corresponding Pt 4f spectra, the peaks representing Pt-CO bonds became more prominent (Figs. S13c and S14). Similar to the phenomenon in pure CO_2, as the temperature went higher to 85 °C, CO desorption dominated during its formation and adsorption processes. The peak intensity for adsorbates began to decline as we further increased the temperature (Fig. 2d). With continued sample heating, RWGS starts at 300 °C, and the production of CO and H_2O grows gradually larger with the rise in temperature (Figs. 2a and S15).

The behavior of the surface graphitic carbon species in the presence of CO_2 and H_2 followed a similar trend to prior results, where Pt was exposed to CO_2 alone. One point should

be noted that there could be some hydrocarbon species formed on the surface in the presence of both CO_2 and H_2 followed by the nucleation, growth and extension of graphitic carbon, which was observed by APXPS on Ir(111) surface[51]. Above 150 °C, the intensity of graphitic carbon starts to decrease (Fig. 2d). In addition to the prior interpretation for the graphitic carbon removal, additional study on CO_2 hydrogenation on an Ir(111) single crystal surface[51] has claimed that, at 330 °C, surface carbon species could be completely reduced or removed by the high H_2 partial pressure in the reaction environment. To evaluate whether the removal of surface graphitic species is promoted by the increase in hydrogen partial pressure or solely by CO_2 serving as an oxidizing agent, we created a surface partially covered by graphitic species using CO_2 gas, removed the CO_2, then exposed the sample to pure H_2 (Fig. S16). Notably, as soon as we introduced H_2 in the system, most of surface CO adsorbates could be blown away by H_2. The intensity of graphitic carbon species kept stable as we heated the sample in pure H_2 atmosphere, indicating the formation of graphitic carbon species are highly related to the existence of CO_2 in our case. However, as soon as we re-dosed CO_2 at 430 °C, the residual graphitic species was removed in less than 1 min. This result is similar to previous APXPS experiments that studied methane reformation with CO_2 on a ZrO_2/Pt(111) model catalyst[52]. Thus, we draw the conclusion that CO_2 plays a critical role in oxidizing and removing the graphitic carbon species at elevated temperatures.

As we further increased the temperature as high as 540 °C, no peak was detectable in the C 1s spectrum, but two new peaks were observed in the O 1s spectrum due to the formation of surface hydroxyl and water species following the RWGS process[53] (Fig. 2c). After the temperature was returned to room temperature, strong CO adsorbate peaks appeared on the surface (Figs. 2b and 2c). Interestingly, another new peak emerged at a binding energy of ~287.8 eV. This has previously been reported to represent CO adsorbates on the top site induced by high CO coverage on the Pt surface[54]. In all the C 1s spectra for the CO experiment, we observed a peak at 287.8 eV (Fig. S17a). By comparing the corresponding C 1s spectra collected in the CO adsorption experiment on oxygen-covered and clean surfaces (Figs. S10 and S17), we established that there was a higher CO surface coverage on the oxygen-free surface (~4.7%) than that on oxygen-rich surface (~2.1%). Therefore, we can rule out the possibility of OCO/COO species, which could be formed through interactions between CO adsorbates and surface oxygen, and thus must be primarily associated with high concentrations of CO adsorbates on the surface.

Interestingly, in the O 1s spectra there is no indication of an additional peak, which suggests that the fitting with two peaks is sufficient (Fig. 2c). In addition, we also noticed that there could be other species such as formate (HCOO) or carboxylic acid (COOH) that were considered as key intermediates in the CO_2 hydrogenation reaction on metal surfaces[27]. However, we cannot assign a peak representing COOH or HCOO based on the obtained C 1s and O 1s spectra. Later, we also checked the literature reporting the APXPS study on HCOOH adsorption on Pt(111) crystals and found that HCOOH is not stable on Pt(111) surface with only CO species observed even at room temperature[48]. Thus, we considered that there could be two possibilities, 1) these species are not forming as part of the reaction pathway, or 2) these intermediates are very short lived on the surface and are not a rate limiting surface reaction process that can be observed during these steady state measurements. This motivates the need for the development of both higher sensitivity detection systems as well as faster time resolved measurements to try and capture these intermediates if they are present. Lastly, additional techniques such as infra-red spectroscopy may be needed to confirm if they exist during the process in the future[20].

3.3. CO_2 adsorption and RWGS on Pt(111) in H_2:CO_2 = 10:1.

Practically, to achieve high CO_2 conversion in the hydrogenation process, we usually apply excess H_2 where the ratio of H_2/CO_2 remained higher than 1[55]. Therefore, the experiment was performed again by exposing the Pt(111) surface to the 1:10 mixture of CO_2 and H_2, resulting in a total pressure of approximately 165 mtorr. In the C 1s and O 1s spectra acquired at room temperature, we could also observe the peaks for CO adsorbed on both top sites and bridge sites (Figs. 3b and 3c). Under these conditions, CO_2 dissociation would occur to produce CO that could also adsorb on the surface. Similar to results for the H_2:CO_2 = 1:1 ratio, exposing the surface to H_2 (~150 mtorr) helped to remove the adsorbed oxygen atoms so that no oxygen atoms were detectable in the O 1s spectra (Figs. 3c and S18b). As the temperature was increased to above 45 ^oC, the surface coverage of CO adsorbates decreased as they began to desorb from the surface (Fig. 3d). The calculated CO coverages in this case were obviously lower than those in the H_2:CO_2 = 1:1 case in all temperature ranges. The reduced CO desorption temperature and lower CO coverage may be due to the reduction of CO by H_2 under the higher H_2 partial pressures, which was also found in an isothermal kinetic study on CO desorption from Pt(111)[56]. As we increased the temperature to 200 ^oC, we observed the onset of the RWGS reaction, as the intensity for CO started to increase in the corresponding mass spectrum (Fig. 3a). At 510 ^oC, as

in the H_2:CO_2 = 1:1 case, the peaks representing surface OH and adsorbed H_2O appeared in the corresponding O 1s spectra as well, due to the formation of H_2O in the system (Fig. 3c). It should be noted that under this condition (H_2:CO_2 > 1:1), researchers expected to obtain the further reduced products such as hydrocarbons and oxygenates based on Pt-based catalysts[57]. Thus, we also tracked the change of the species representing methane in our mass spectra (Fig. S20). The intensity change for methane was in the magnitude of 10^{-10} torr, which was too small to be considered as the formation of methane as a product in our system. Graphitic carbon species, in this case, behaved a little differently from the first two cases as we increased the temperature. As we heated the Pt from 65 to 150 °C, the coverage of graphitic carbon soared from 0.03 ML to 0.12 ML. The coverage of graphitic carbon remained largely unchanged as the temperature was increased to 200 °C (Fig. 3d), unlike results from the H_2:CO_2 = 1:1 case, where the surface coverage of graphitic carbon was reduced significantly over the same temperature range. As we dosed H_2 with higher partial pressure, more CO adsorbates were further hydrogenated, leading to the generation of more graphitic carbon species on the surface. It should be noted that in practical catalytic reactions, the formation of graphitic carbon on the surface (or coke formation) is usually considered as the poisoning of catalysts, leading to the deactivation. The metal-support interaction proves to be of great help to suppress the graphitic carbon formation. To approach the practical catalytic environment, in future studies we will explore the metal-support interaction to further understand how this can help to suppress or remove carbon depositions[58].

3.4. Direct comparison of the three conditions.

To compare overall CO_2 surface reactions on Pt(111) under the three different atmospheres, we calculated the CO_2 conversion, as well as the production of CO and H_2O, at various reaction conditions (Fig. 4). CO and H_2O pressure was calibrated based on the standard curve obtained from the controlled experiment conducted in the same system (Fig. S5). In the presence of pure CO_2, the conversion of CO_2 rose from 0.05 to 0.36% as the temperature increased from 300 to 540 °C, in accordance with the endothermic properties of CO_2 dissociation[43]. After H_2 was introduced into the system, we observed more apparent production of CO and H_2O from the conversion of CO_2 (Figs. 4a and 4b). Considering the thermodynamic properties of the RWGS[59], the highest CO_2 conversion (~9.5%) was achieved under the condition of H_2:CO_2 = 10:1 at 510 °C (Fig. 4a). Notably, the pressure of CO_2 gas is different under various pressure of H_2:CO_2. In detail, 40 mtorr of CO_2 was dosed in H_2:CO_2 = 1:1 while 15 mtorr of CO_2 was introduced in the

case of H_2:CO_2 = 10:1 because of the limitation of our APXPS system. Therefore, we obtained a much higher CO_2 conversion in H_2:CO_2 = 10:1 with similar amount of products (Fig. 4b). Furthermore, a specific spectrum comparison of the behavior at 200 °C under the three conditions is shown in Fig. S21. In pure CO_2, the C 1s spectrum contained only a slight feature representing CO adsorbates on top sites of the surface; this feature was also observed in the O 1s spectrum, in addition to adsorbed oxygen atoms on the surface (Fig. S21). When H_2 was included, we found more obvious CO adsorbates in both C 1s and O 1s spectra, indicating that more CO formed at 200 °C under both H_2:CO_2 = 1:1 and H_2:CO_2 = 10:1 conditions compared with amounts in pure CO_2.

To more clearly elucidate the surface reaction process at the interface, a schematic illustration is provided in Fig. 5. At room temperature, CO_2 dissociation should be the dominant process under the conditions we set in the experiment. Consequently, we can see the adsorbed CO as well as adsorbed oxygen atoms on the surface in pure CO_2. When H_2 was included, adsorbed oxygen could be removed by dissociated H atoms from hydrogen at room temperature. CO desorption accelerated as the temperature rose, and therefore the peak intensity of CO adsorbates was lower. At temperatures above 150 °C, surface graphitic carbon can be oxidized by CO_2; the peak intensity for graphitic carbon dropped as a result. As is well established, high temperature favors endothermic reactions, including both CO_2 dissociation and RWGS. Due to the high reaction rate and desorption rate, surface carbon species were completely removed. More CO was observed in the gaseous phase at temperatures over 450 °C for the pure CO_2 case, whereas the production of CO and H_2O became more obvious in mass spectra at temperatures over 300 °C in the case where H_2:CO_2 = 1:1 and over 200 °C for H_2:CO_2 = 10:1.

4. Conclusion

In summary, our APXPS study provides detailed insights into the surface changes and production selectivity on a Pt(111) surface in the presence of pure CO_2 or CO_2 + H_2 in the mtorr range. With pure CO_2 gas, we find clear evidence for the formation of surface atomic oxygen on the Pt surface, indicating that CO_2 dissociation proceeds even at room temperature. Due to the strong binding between CO and Pt, surface CO adsorbates were easily observed as well. Elevated temperatures can accelerate the CO_2 dissociation rate on Pt(111), as confirmed by the increased peak intensity for surface oxygen. This experiment provides evidence that CO_2 dissociation can

occur under sufficiently high-pressure conditions even at room temperature, which was seldom considered in previous literature[16,17]. In addition, graphitic carbon species form on the surface, and the intensity rises with an increase from room temperature to 150 °C. At temperatures higher than 150 °C, graphitic carbon can be oxidized by CO_2 following the reverse Boudouard Reaction. Adding the same amount of H_2 into the system promotes CO_2 dissociation to generate more CO adsorbates on the Pt(111) surface; at 300 °C, the RWGS reaction begins, producing CO and H_2O. With excess H_2 dosed into the system (H_2:CO_2 = 10:1), the RWGS becomes dominant from temperatures as low as 200 °C, due to the high H_2 partial pressure. This work delivers a systematic investigation of CO_2 hydrogenation on crystalline Pt and advances our understanding of the mechanism of CO_2 hydrogenation to form CO and H_2O, guiding optimal design of future catalysts.

Appendix A. Supplementary material. The supporting information including following files is available free of charge online at DOI: XXX.

Author Contributions

The manuscript was written with contributions from all authors. H.S. and E. J. C designed the experiments. H. S., Y. Y., and K.-J. L performed the APXPS experiment. H. S. analyzed the data and wrote the manuscript. All authors have given approval to the final version of the manuscript.

Declaration of Competing Interest

The authors declare that they have no known competing financial interests or personal relationships that could have appeared to influence the work reported in this paper.

Acknowledgement

The research used resources of the Advanced Light Source, which is a DOE Office of Science User Facility under contract no. DE-AC02-05CH11231. H.S. gratefully acknowledges the China Scholarship Council (CSC, No. 201706340112) for financial support. Y.Y. and E.J.C. were partially supported by an Early Career Award in the Condensed Phase and Interfacial

Molecular Science Program, in the Chemical Sciences Geosciences and Biosciences Division of the Office of Basic Energy Sciences of the U.S. Department of Energy under Contract No. DE-AC02-05CH11231.

Reference

[1] M. D. Porosoff, B. Yan, J. G. Chen, Catalytic reduction of CO_2 by H_2 for synthesis of CO, methanol and hydrocarbons: challenges and opportunities. Energy Environ. Sci. 9 (2016) 62-73.

[2] W.-H. Wang, Y. Himeda, J. T. Muckerman, G. F. Manbeck, E. Fujita, CO_2 Hydrogenation to Formate and Methanol as an Alternative to Photo- and Electrochemical CO_2 Reduction. Chem. Rev. 115 (2015) 12936-12973.

[3] J. Jia, C. Qian, Y. Dong, Y. F. Li, H. Wang, M. Ghoussoub, K. T. Butler, A. Walsh, G. A. Ozin, Heterogeneous catalytic hydrogenation of CO_2 by metal oxides: defect engineering-perfecting imperfection. Chem. Soc. Rev.46 (2017) 4631-4644.

[4] J. Wei, Q. Ge, R. Yao, Z. Wen, C. Fang, L. Guo, H. Xu, J. Sun, Directly converting CO_2 into a gasoline fuel. Nat. Commun. 8 (2017) 15174.

[5] W. Wang, S. Wang, X. Ma, J. Gong, Recent advances in catalytic hydrogenation of carbon dioxide. Chem. Soc. Rev. 40 (2011) 3703-3727.

[6] M. D. Porosoff, J. G. Chen, Trends in the catalytic reduction of CO_2 by hydrogen over supported monometallic and bimetallic catalysts, J. Catal. 301 (2013) 30-37.

[7] Y. A. Daza, J. N. Kuhn, CO_2 conversion by reverse water gas shift catalysis: comparison of catalysts, mechanisms and their consequences for CO_2 conversion to liquid fuels. RSC Adv. 6 (2016) 49675-49691.

[8] K. Oshima, T. Shinagawa, Y. Nogami, R. Manabe, S. Ogo, Y. Sekine, Low temperature catalytic reverse water gas shift reaction assisted by an electric field. Catalysis Today 232 (2014) 27-32.

[9] H. Li, L. Wang, Y. Dai, Z. Pu, Z. Lao, Y. Chen, M. Wang, X. Zheng, J. Zhu, W. Zhang, et al. Synergetic interaction between neighboring platinum monomers in CO_2 hydrogenation. Nat. Nanotechnol. 13 (2018) 411-417.

[10] M. C. Roman-Martinez, D. Cazorla-Amoros, C. Salinas-Martinez de Lecea, A. Linares-Solano, Structure Sensitivity of CO_2 Hydrogenation Reaction Catalyzed by Pt/Carbon Catalysts. Langmuir 12 (1996) 379-385.

[11] K. Dhar, C. Cavallotti, Investigation of the Initial Steps of the Electrochemical Reduction of CO_2 on Pt Electrodes. J. Phys. Chem. A 118 (2014) 8676-8688.

[12] L. Dietz, S. Piccinin, M. Maestri, Mechanistic Insights into CO_2 Activation via Reverse Water-Gas Shift on Metal Surfaces. J. Phys. Chem. C 119 (2015) 4959-4966.

[13] S. Kattel, B. Yan, J. G. Chen. P. Liu, CO_2 hydrogenation on Pt, Pt/SiO_2 and Pt/TiO_2: Importance of synergy between Pt and oxide support. J. Catal. 343 (2016) 115-126.

[14] C. Shi, C. P. O'Grady, A. A. Peterson, H. A. Hansen, J. K. Norskov, Modeling CO_2 reduction on Pt(111). Phys. Chem. Chen. Phys. 15 (2013) 7114-7122.

[15] A. Goguet, F. C. Meunier, D. Tibiletti, J. P. Breen, R. Bruch, Spectrokinetic Investigation of Reverse Water-Gas-Shift Reaction Intermediates over a Pt/CeO_2 Catalyst. J. Phys. Chem. B 108 (2014) 20240-20246.

[16] Z. M. Liu, Y. Zhou, F. Solymosi, J. M. White, Spectroscopic study of K-induced activation of CO_2 on Pt(111). Surf. Sci. 245 (1991) 289-304.

[17] M. Huang, A. Adnot, S. Suppiah, S. Kaliaguine, XPS observation of surface interaction between H_2 and CO_2 on platinum foil. J. Mol. Catal. A Chem. 104 (1995) L131-L137.

[18] F. Tao, M. E. Grass, Y. Zhang, D. R. Butcher, J. R. Renzas, Z. Liu, J. Y. Chung, B. S. Mun, M. Salmeron, G. A. Somorjai, Reaction-Driven Restructuring of Rh-Pd and Pt-Pd Core-Shell Nanoparticles. Science 322 (2008) 932-934.

[19] M. Salmeron, R. Schlögl, Ambient pressure photoelectron spectroscopy: A new tool for surface science and nanotechnology. Surf. Sci. Rep. 63 (2008) 169-199.

[20] J. Graciani, K. Mudiyanselage, F. Xu, A. E. Baber, J. Evans, S. D. Senanayake, D. J. Stacchiola, P. Liu, J. Hrbek, J. Fernández Sanz, et al. Highly active copper-ceria and copper-ceria-titania catalysts for methanol synthesis from CO_2. Science 345 (2014) 546-550.

[21] F. Jiao, J. Li, X. Pan, J. Xiao, H. Li, H. Ma, M. Wei, Y. Pan, Z. Zhou, M. Li, et al. Selective conversion of syngas to light olefins. Science 351 (2016) 1065-1068.

[22] M. E. Grass, P. G. Karlsson, F. Aksoy, M. Lundqvist, B. Wannberg, B. S. Mun, Z. Hussian, Z. Liu, New ambient pressure photoemission endstation at Advanced Light Source beamline 9.3.2. Rev. Sci. Instrum. 81 (2010) 053106.

[23] T. Schiros, L.-Å. Näslund, K. Andersson, J. Gyllenpalm, G. S. Karlberg, M. Odelius, H. Ogasawara, L. G. M. Pettersson, A. Nilsson, Structure and Bonding of the Water-Hydroxyl Mixed Phase on Pt(111). J. Phys. Chem. C 111 (2007) 15003-15012.

[24] C. H. Wu, B. Eren, H. Bluhm, M. Salmeron, Ambient-Pressure X-ray Photoelectron Spectroscopy Study of Cobalt Foil Model Catalyst under CO, H_2, and Their Mixtures. ACS Catal. 7 (2017) 1150-1157.

[25] J. T. Newberg, D. E. Starr, S. Yamamoto, S. Kaya, T. Kendelewicz, E. R. Mysak, S. Porsgaard, M. B. Salmeron, G. E. Brown Jr, A. Nilsson, H. Bluhm, Formation of hydroxyl and water layers on MgO films studied with ambient pressure XPS. Surf. Sci. 605 (2011) 89-94.

[26] R. Toyoshima, M. Yoshida, Y. Monya, K. Suzuki, K. Amemiya, K. Mase, B. S. Mun, H. Kondoh, A High-pressure-induced Dense CO Overlayer on a Pt(111) Surface: A Chemical Analysis Using in situ Near Ambient Pressure XPS. Phys. Chem. Chem. Phys. 16 (2014) 23564-23567.

[27] M. Roiaz, E. Monachino, C. Dri, M. Greiner, A. Knop-Gericke, R. Schlogl, G. Comelli, E. Vesselli, Reverse Water–Gas Shift or Sabatier Methanation on Ni(110)? Stable Surface Species at Near-Ambient Pressure. J. Am. Chem. Soc. 138 (2016) 4146-4154.

[28] M. Kinne, T. Fuhrmann, C. M. Whelan, J. F. Zhu, J. Pantforder, M. Probst, G. Held, R. Denecke, H.-P. Steinruck, Kinetic Parameters of CO Adsorbed on Pt(111) Studied by in situ High Resolution X-ray Photoelectron Spectroscopy. J. Chem. Phys. 117 (2002) 10852-10859.

[29] J. C. Fuggle, E. Umbach, D. Menzel, K. Wandelt, C. R. Brundle, Adsorbate line shapes and multiple lines in XPS: comparison of theory and experiment. Solid State Commun. 27 (1978) 65-69.

[30] B. Gumhalter, K. Wandelt, $2\pi^*$ resonance features in the electronic spectra of chemisorbed CO. Phys. Rev. B 37 (1988) 8048-8065.

[31] I. Píš, E. Magnano, S. Nappini, F. Bondino, Under-cover stabilization and reactivity of a dense carbon monoxide layer on Pt(111). Chem. Sci. 10 (2019) 1857-1865.

[32] Y. Yao, Q. Fu, Y. Y. Zhang, X. Weng, H. Li, M. Chen, L. Jin, A. Dong, R. Mu, P. Jiang, et al. Graphene cover-promoted metal-catalyzed reactions. Proc. Natl. Acad. Sci. U.S.A., 111 (2014) 17023-17028.

[33] R. Blume, D. Rosenthal, J.-P. Tessonnier, H. Li, A. Knop-Gericke, R. Schlögl. Characterizing Graphitic Carbon with X-ray Photoelectron Spectroscopy: A Step-by-Step Approach. ChemCatChem 7 (2015) 2871-2881.

[34] D. R. Butcher, M. E. Grass, Z. Zeng, F. Aksoy, H. Bluhm, W.-X. Li, B. S. Mun, G. A. Somorjai, Z. Liu, In Situ Oxidation Study of Pt(110) and Its Interaction with CO. J. Am. Chem. Soc. 133 (2011) 20319-20325.

[35] J. Kim, W. H. Park, W. H. Doh, S. W. Lee, M. C. Noh, J.-J. Gallet, F. Bournel, H. Kondoh, K. Mase, Y. Jung, et al. Adsorbate-driven reactive interfacial Pt-NiO_{1-x} nanostructure formation on the $Pt_3Ni(111)$ alloy surface. Sci. Adv. 4 (2018) eaat3151.

[36] A. C. Luntz, J. Grimblot, Fowler, D. E. Sequential precursors in dissociative chemisorption: O_2 on Pt(111). Phys. Rev. B 39 (1989) 12903.

[37] B. Shan, N. Kapur, J. Hyun, L. Wang, J. B. Nicholas, K. Cho, CO-Coverage-Dependent Oxygen Dissociation on Pt(111) Surface. J. Phys. Chem. C 113 (2009) 710-715.

[38] M. M. Montemore, M. A. van Spronsen, R. J. Madix, C. M. Friend, O_2 Activation by Metal Surfaces: Implications for Bonding and Reactivity on Heterogeneous Catalysts. Chem. Rev. 118 (2018) 2816-2862.

[39] D. J. Miller, H. Oberg, S. Kaya, H. Sanchez Casalongue, D. Friebel, T. Anniyev, H. Ogasawara, H. Bluhm, L. G. M. Pettersson, A. Nilsson, Oxidation of Pt(111) under Near-Ambient Conditions. Phys. Rev. Lett. 107 (2011) 195502.

[40] F. Tao, S. Dag, L.-W. Wang, Z. Liu, D. R. Butcher, H. Bluhm, M. Salmeron, G. A. Somorjai, Break-Up of Stepped Platinum Catalyst Surfaces by High CO Coverage. Science, 327 (2010) 850-853.

[41] S. R. Longwitz, J. Schnadt, E. K. Vestergaard, R. T. Vang, I. Stensgaard, H. Brune, F. Besenbacher, High-Coverage Structures of Carbon Monoxide Adsorbed on Pt(111) Studied by High-Pressure Scanning Tunneling Microscopy. J. Phys. Chem. B 108 (2004) 14497-14502.

[42] S. K. Jo, Weakly-bound Hydrogen on Defected Pt(111), Surf. Sci. 635 (2015) 99-107.

[43] X. Liu, L. Sun, W.-Q. Deng, Theoretical Investigation of CO_2 Adsorption and Dissociation on Low Index Surfaces of Transition Metals. J. Phys. Chem. C 122 (2018) 8306-8314.

[44] M. Hecq, A. Hecq, J. P. Delrue, T. Robert, Sputtering Deposition, XPS and X-Ray Diffraction Characterization of Oxygen-Platinum Compounds. J. Less-Common Met. 64 (1979) P25-P37.

[45] K. Ding, A. Gulec, A. M. Johnson, N. M. Schweitzer, G. D. Stucky, L. D. Marks, P. C. Stair, Identification of active sites in CO oxidation and water-gas shift over supported Pt catalysts. Science 350 (2015) 189-192.

[46] M. Favaro, H. Xiao, T. Cheng, W. A. Goddard III, J. Yano E. J. Crumlin, Subsurface oxide plays a critical role in CO_2 activation by Cu(111) surfaces to form chemisorbed CO_2, the first step in reduction of CO_2. Proc. Natl. Acad. Sci. U.S.A. 114 (2017) 6706-6711.

[47] Y. Ye, H. Yang, J. Qian, H. Su, K.-J. Lee, T. Cheng, H. Xiao, J. Yano, W. A. Goddard III, E. J. Crumlin, Dramatic differences in carbon dioxide adsorption and initial steps of reduction between silver and copper. Nat. Commun. 10 (2019) 1875.

[48] B. Jeong, H. Jeon, R. Toyoshima, E. J. Crumlin, H. Kondoh, B. S. Mun, J. Lee, Dehydration Pathway for the Dissociation of Gas-Phase Formic Acid on Pt(111) Surface Observed via Ambient-Pressure XPS. J. Phys. Chem. C 122 (2018) 2064-2069.

[49] D. E. Starr, H. Bluhm, CO adsorption and dissociation on Ru(0001) at elevated pressures. Surf. Sci. 608 (2013) 241-248.

[50] J. Hunt, A. Ferrari, A. Lita, M. Crosswhite, B. Ashley, A. E. Stiegman, Microwave-Specific Enhancement of the Carbon-Carbon Dioxide (Boudouard) Reaction. J. Phys. Chem. C 117 (2013) 26871-26880.

[51] M. Corva, Z. Feng, C. Dri, F. Salvador, P. Bertoch, G. Cornelli, E. Vesselli, Carbon Dioxide Reduction on Ir(111): Stable Hydrocarbon Surface Species at Near-ambient Pressure. Phys. Chem. Chem. Phys. 18 (2016) 6763-6772.

[52] C. Rameshan, H. Li, K. Anic, M. Roiaz, V. Pramhaas, R. Rameshan, R. Blume, M. Hävecker, J. Knudsen, A. Knop-Gericke, et al. In situ NAP-XPS spectroscopy during methane dry reforming on ZrO_2/Pt(111) inverse model catalyst. J. Phys.: Condens. Matter 30 (2018) 264007.

[53] C. Heine, B. A. Lechner, H. Bluhm, M. Salmeron, Recycling of CO_2: Probing the Chemical State of the Ni(111) Surface during the Methanation Reaction with Ambient-Pressure X-Ray Photoelectron Spectroscopy. J. Am. Chem. Soc. 138 (2016) 13246-13252.

[54] J. F. Zhu, M. Kinne, T. Fuhrmann, B. Tränkenschuh, R. Denecke, H. P. Steinrück, in Surface Science, New Research, edited by C. P. Norris (Nova Science, Hauppauge, NY, 2005), p. 217.

[55] S. Kattel, P. Liu, J. G. Chen, Tuning Selectivity of CO_2 Hydrogenation Reactions at the Metal/Oxide Interface. J. Am. Chem. Soc. 139 (2017) 9739-9754.

[56] D. H. Parker, D. A. Fisher, J. Colbert, B. E. Koel, J. L. Gland, Hydrogen-induced CO displacement from Pt(111) surface: an isothermal kinetic study. Surf. Sci. 258 (1991)75-81.

[57] K.-P. Yu, W.-Y. Yu, M.-C. Kuo, Y.-C. Liou, S.-H. Chien, Pt/titania-nanotube: A potential catalyst for CO_2 adsorption and hydrogenation. Appl. Catal. B 84 (2008) 112-118.

[58] A. Bruix, J. A. Rodriguez, P. J. Ramírez, S. D. Senanayake, J. Evans, J. B. Park, D. Stacchiola, P. Liu, J. Hrbek, F. Illas, A New Type of Strong Metal-Support Interaction and the Production of H_2 through the Transformation of Water on $Pt/CeO_2(111)$ and $Pt/CeO_x/TiO_2(110)$ Catalysts. J. Am. Chem. Soc. 134 (2012) 8968-8974.

[59] J. Artz, T. E. Müller, K. Thenert, Sustainable Conversion of Carbon Dioxide: An Integrated Review of Catalysis and Life Cycle Assessment. Chem. Rev. 118 (2018) 434-504.

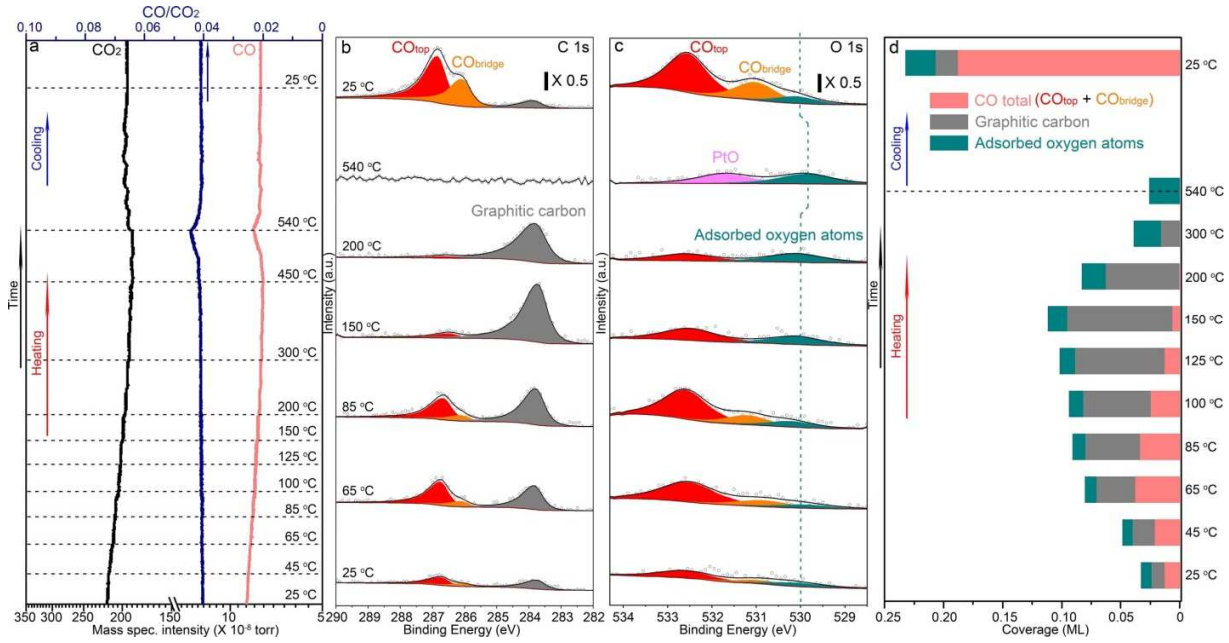

Figure 1. (a) Mass spectra, (b) C 1s spectra, and (c) O 1s spectra collected in the presence of CO_2 at different temperatures. (d) Peak trend for CO adsorbates and surface oxygen species according to the XPS spectra. The sample was heated from 25 ºC to 540 ºC followed by cooling to room temperature (25 ºC). The navy curve in (a) represents the ratio of CO and CO_2 as a function of time. All spectra were fitted with LA line shape (asymmetric) after applying the Shirley background.

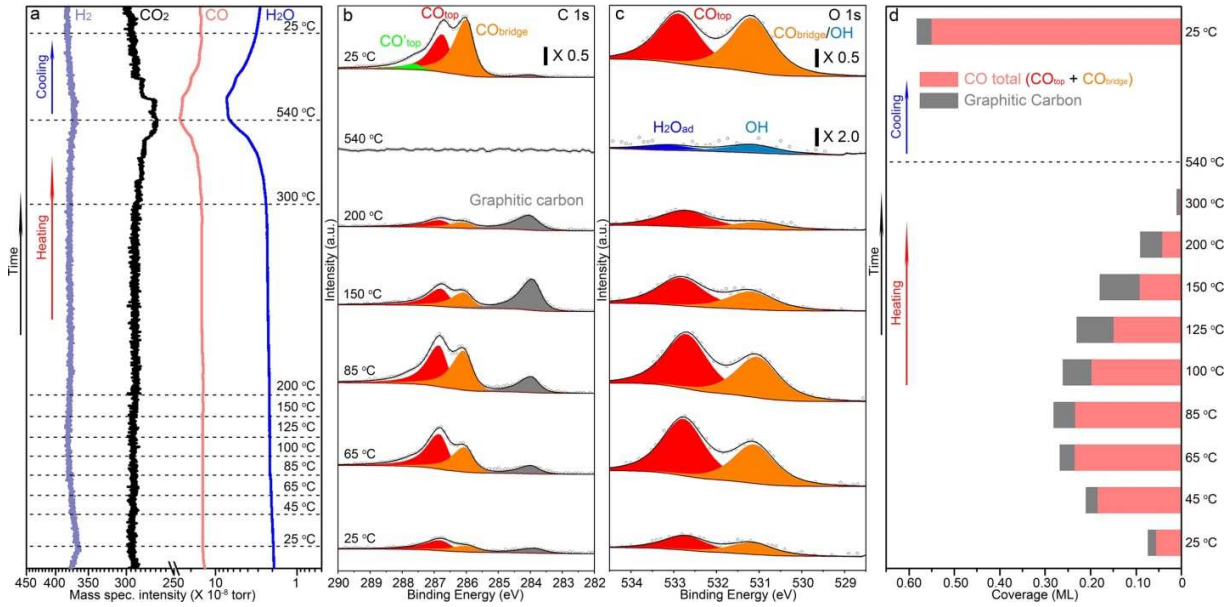

Figure 2. (a) Mass spectra, (b) C 1s spectra, and (c) O 1s spectra collected in the presence of CO_2 and H_2 (H_2:CO_2 = 1:1) at different temperatures. (d) Peak trend for CO adsorbates and surface graphitic carbon species according to the XPS spectra. The sample was heated from 25 ºC to 540 ºC followed by cooling to room temperature (25 ºC). All the spectra were fitted with LA line shape (asymmetric) after applying the Shirley background.

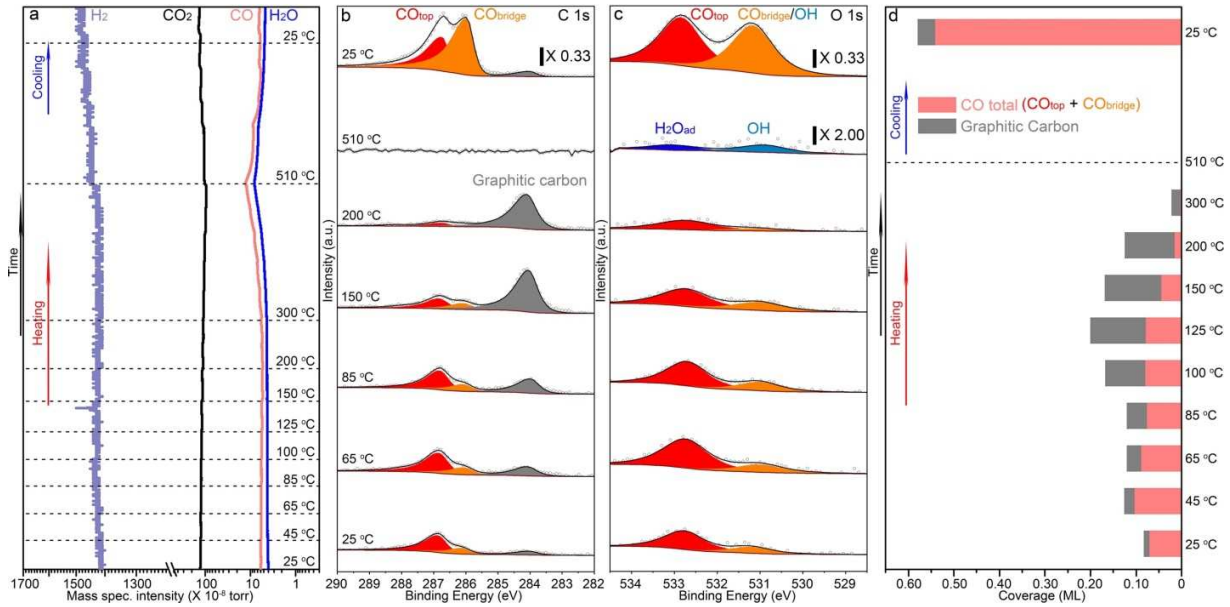

Figure 3. (a) Mass spectra, (b) C 1s spectra, and (c) O 1s spectra collected in the presence of CO_2 and H_2 (H_2:CO_2 = 10:1) at different temperatures. (d) Peak trend for CO adsorbates and surface graphitic carbon species according to the XPS spectra. The sample was heated from 25 °C to 510 °C followed by cooling to room temperature (25 °C). All the spectra were fitted with LA line shape (asymmetric) after applying the Shirley background.

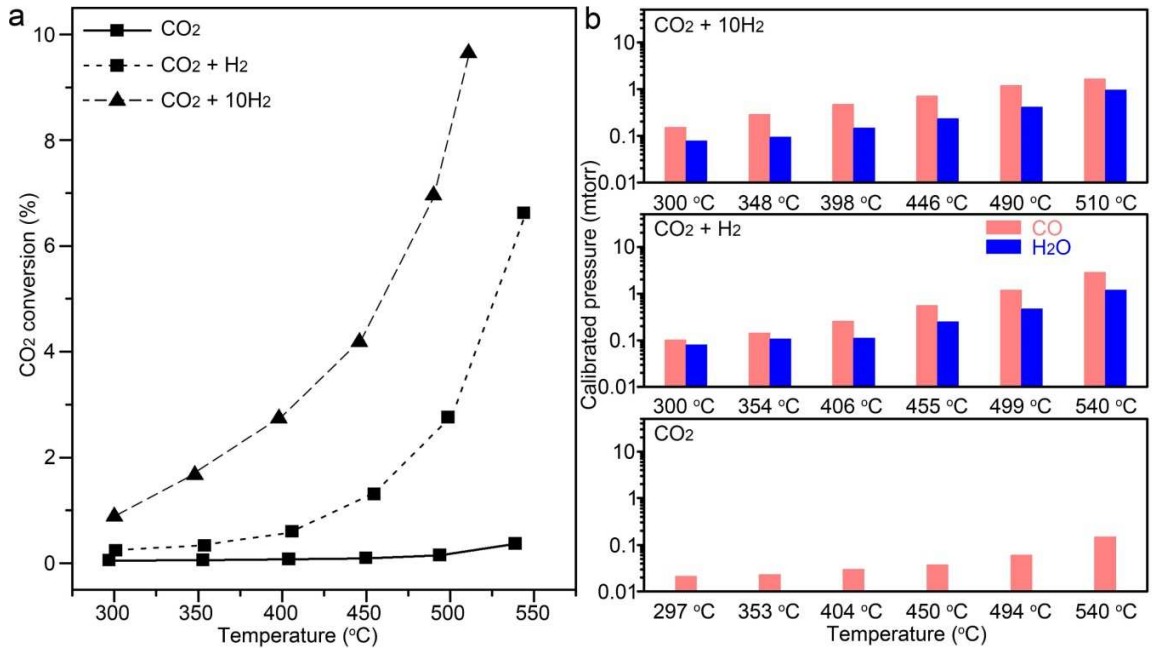

Figure 4. (a) CO_2 conversion percentage under different conditions and (b) corresponding production amounts for CO and H_2O after mass spectra calibration.

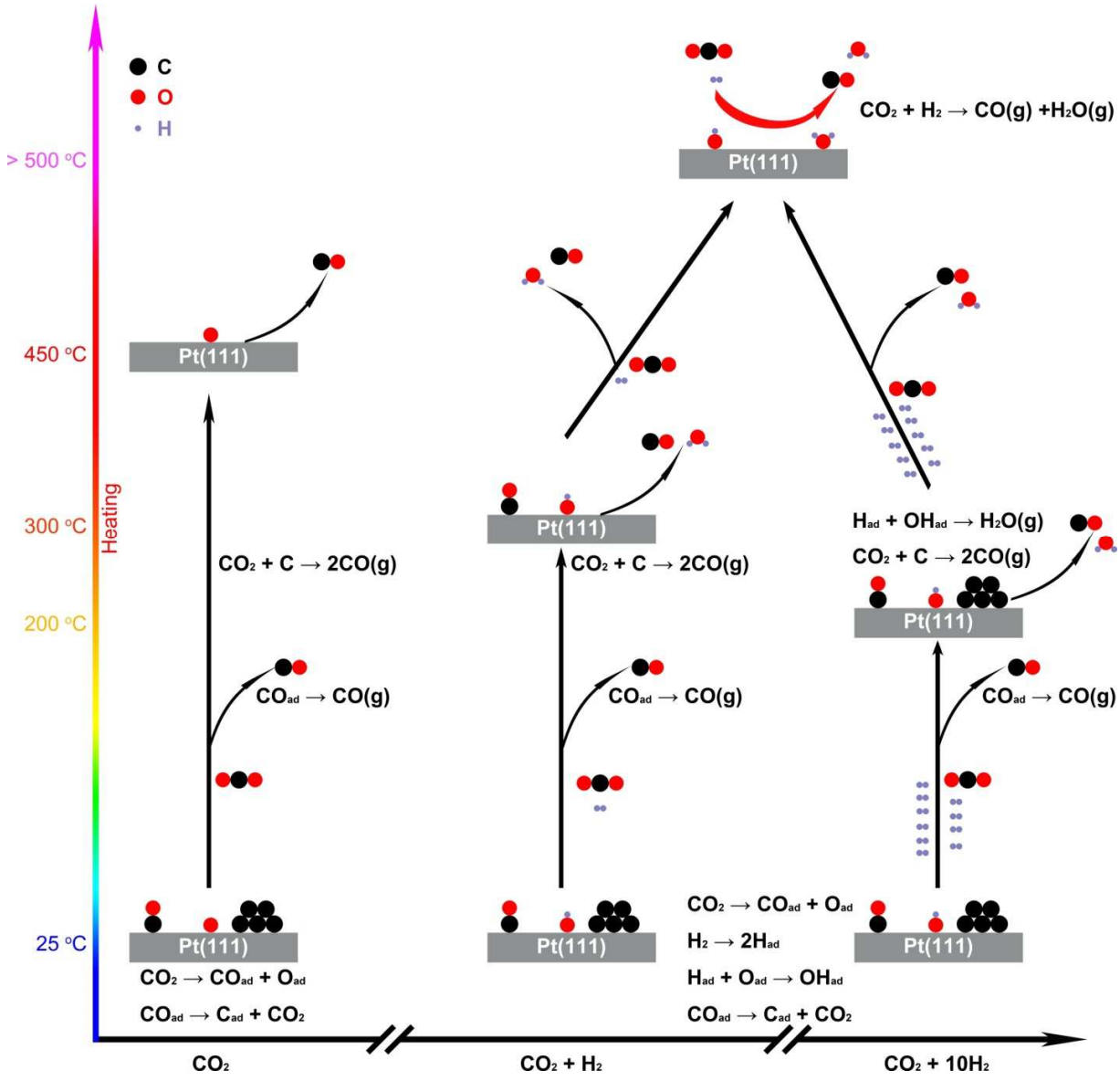

Figure 5. Schematic illustration showing the entire process of CO_2 activation and conversion under three different conditions. The spheres in various colors represent C (black), O (red), and H (violet) atoms, respectively.

TOC Graphic

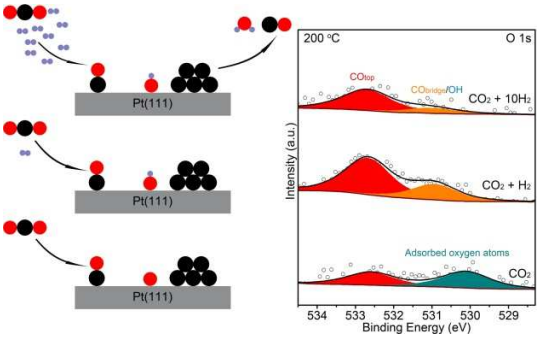
Pt(111)
Pt(111)
Pt(111)
200 °C
O 1s
CO$_{top}$
CO$_{bridge}$/OH
CO$_2$ + 10H$_2$
CO$_2$ + H$_2$
Adsorbed oxygen atoms
CO$_2$
Intensity (a.u.)
534
533
532
531
530
529
Binding Energy (eV)